
**UNIVERSITI PUTRA MALAYSIA**

***THE INFLUENCE OF TEMPERATURE ON OPTICAL, STRUCTURAL AND MORPHOLOGICAL PROPERTIES OF COPPER HEXADECAFLUORO PHTHALOCYANINE (F16CuPc) THIN FILMS***

**NUR AFIQAH BINTI NIZAMMESRASURIA**

# THE INFLUENCE OF TEMPERATURE ON OPTICAL, STRUCTURAL AND MORPHOLOGICAL PROPERTIES OF COPPER HEXADECAFLUORO PHTHALOCYANINE ($F_{16}CuPc$) THIN FILMS

**NUR AFIQAH BINTI NIZAMMESRASURIA**

**BACHELOR OF SCIENCE IN PHYSICS WITH EDUCATION (HONOURS)**

**UNIVERSITI PUTRA MALAYSIA**

**2022**

# THE INFLUENCE OF TEMPERATURE ON OPTICAL, STRUCTURAL AND MORPHOLOGICAL PROPERTIES OF COPPER HEXADECAFLUORO PHTHALOCYANINE ($F_{16}CuPc$) THIN FILMS

**By**

**NUR AFIQAH BINTI NIZAMMESRASURIA**

**Thesis Submitted to the Department of Physics, Universiti Putra Malaysia in Partial Fulfilment of the Requirements for the Bachelor of Science in Physics with Education (Honours)**

**February 2022**

Abstract of thesis presented to the Department of Physics, Faculty of Science, Universiti Putra Malaysia in fulfilment of the requirement for the Bachelor of Science in Physics with Education (Honours)

# THE INFLUENCE OF TEMPERATURE ON OPTICAL, STRUCTURAL AND MORPHOLOGICAL PROPERTIES OF COPPER HEXADECAFLUORO PHTHALOCYANINE ($F_{16}CuPc$) THIN FILMS

By

**NUR AFIQAH BINTI NIZAMMESRASURIA**

**February 2022**

**Supervisor: Nur Adilah Binti Roslan, PhD**
**Faculty: Faculty of Science**

In this study, a metal phthalocyanine (MPc), copper hexadecafluoro phthalocyanine ($F_{16}CuPc$) thin films are deposited and studied to observe the effects of thermal annealing on them. This study is done to identify the optical, structural and morphological properties of $F_{16}CuPc$ thin films by varying thermal annealing. $F_{16}CuPc$ thin films have been deposited on glass substrates using thermal evaporation method and are annealed to 50 °C, 100 °C, and 200 °C. Using UV-Vis-NIR spectrometer, the results show that $F_{16}CuPc$ thin films are well absorbing in the ultraviolet (UV) and visible (Vis) range, with two sharp peaks at 360 nm and 789 nm with a shoulder at 650 nm, corresponds to $\pi$-$\pi^*$ transitions, respectively. This study proves no significant effect on varied temperature for optical properties of $F_{16}CuPc$ thin films. The $F_{16}CuPc$ thin films are suitable for light sensing application as they presented a high extinction coefficient in the Vis region. The

optical band gap energy, $E_g$ gained from the Tauc's equation is $(3.04 \pm 0.01)$ eV, which is close enough to the value gained by extrapolating the plot of absorbance to the horizontal axis, 2.97 eV. Structural properties are also studied using (X-ray Diffraction) XRD analysis, which shows the $F_{16}CuPc$ powder is in the crystallized phase. However, the study depicts an amorphous phase for annealed $F_{16}CuPc$ thin films, which contradicts to the previous researches. This is due to low optimization during the deposition process since there is no indicator to indicate the deposition rate and the distance between the source and substrates. Despite the failure to get the expected result for the structural properties, the morphological properties of $F_{16}CuPc$ thin films by Atomic Force Microscopy (AFM) show that the surface's roughness increases as the annealing temperature increases. The effects of thermal annealing on optical, structural and morphological properties of $F_{16}CuPc$ thin films are explained in this work.

Abstrak thesis yang dikemukan kepada Jabatan Fizik, Fakulti Sains, Universiti Putra Malaysia sebagai memenuhi keperluan untuk Bacelor Sains dengan Pendidikan (Kepujian) Fizik

**PENGARUH SUHU KE ATAS SIFAT OPTIK, STRUKTUR DAN MORFOLOGI TERHADAP FILEM NIPIS KUPRUM HEKSADEKAFLUORO PHTHALOCYANINE ($F_{16}$CuPc)**

Oleh

**NUR AFIQAH BINTI NIZAMMESRASURIA**

**Februari 2022**

**Penyelia: Nur Adilah Binti Roslan, PhD**
**Fakulti: Fakulti Sains**

Dalam kajian ini, filem nipis logam phthalocyanine (MPc), kuprum heksadekafluoro phthalocyanine ($F_{16}$CuPc) dimendapkan dan dikaji untuk melihat kesan penyepuhlindapan haba ke atasnya. Kajian ini dilakukan untuk mengenal pasti sifat optik, struktur dan morfologi filem nipis $F_{16}$CuPc dengan mempelbagaikan penyepuhlindapan haba. Filem nipis $F_{16}$CuPc telah dimendapkan pada substrat kaca menggunakan kaedah penyejatan terma dan disepuhlindapkan kepada 50 °C, 100 °C, dan 200 °C. Menggunakan spektrometer UV-Vis-NIR, keputusan menunjukkan bahawa filem nipis $F_{16}$CuPc menyerap dengan baik dalam julat ultraungu (UV) dan boleh dilihat (Vis), dengan dua puncak tajam pada 360 nm dan 789 nm dengan bahu pada 650 nm, sepadan dengan $\pi$-$\pi^*$ peralihan. Kajian ini membuktikan tiada kesan yang signifikan terhadap suhu yang berbeza-beza untuk sifat optik filem nipis $F_{16}$CuPc. Filem nipis $F_{16}$CuPc sesuai untuk

aplikasi penderiaan cahaya kerana ia menunjukkan pekali kepupusan yang tinggi di rantau Vis. Tenaga jurang jalur optik, $E_g$ yang diperoleh daripada persamaan Tauc ialah $(3.04 \pm 0.01)$ eV, yang cukup hampir dengan nilai yang diperoleh dengan mengekstrapolasi plot penyerapan kepada paksi mendatar, 2.97 eV. Sifat struktur juga dikaji menggunakan analisis *X-ray Diffraction* (XRD), yang menunjukkan serbuk $F_{16}$CuPc berada dalam fasa terhablur. Walau bagaimanapun, kajian itu menggambarkan fasa amorfus untuk filem nipis $F_{16}$CuPc anil, yang bercanggah dengan penyelidikan terdahulu. Ini disebabkan oleh pengoptimuman yang rendah semasa proses pemendapan kerana tiada penunjuk untuk menunjukkan kadar pemendapan dan jarak antara sumber dan substrat. Walaupun kegagalan untuk mendapatkan hasil yang diharapkan untuk sifat struktur, sifat morfologi filem nipis $F_{16}$CuPc oleh *Atomic Force Microscopy* (AFM) menunjukkan bahawa kekasaran permukaan meningkat apabila suhu penyepuhlindapan meningkat. Kesan penyepuhlindapan haba pada sifat optik, struktur dan morfologi filem nipis $F_{16}$CuPc dijelaskan dalam kerja ini.

## ACKNOWLEDGEMENTS

Throughout the writing of this dissertation, I have gained a lot of support and assistance. I would like first to express my deep gratitude to my supervisor, Dr. Adilah Binti Roslan, for her continuous guidance in my Final Year Project. I thank her for all the critical advice and help to encourage me to complete the dissertation.

I sincerely express my gratitude to Dr. Tan Sin Tee, Dr. Josephine Liew Ying Chyi, and Low Yiin Jian for their ideas and assistance in the laboratory.

I am thankful to every staff member of the Physics Department in the Faculty of Science, Universiti Putra Malaysia, for the invaluable help.

I am genuinely thankful to the Low Dimensional Material Research Centre (LDMRC) team, Physics Department, Faculty of Science, Universiti Malaya for the great help.

I express my sincere thanks to my Final Year Project team members, Muhammad Izzudin Bin Mohd Najib and Amirul Mirza Fahmi Bin Shamsuri for their ideas and opinions.

My sincere gratitude goes to my lovely parents, Nizammesrasuria Bin Abdullah and Maziah Binti Mohmin and my roommate, Farah Hananni Binti Haidzir, for the motivational support. Thank you all.

## LIST OF TABLES

## LIST OF FIGURES

## LIST OF ABBREVATIONS

| | |
|---|---|
| $F_{16}CuPc$ | Copper Hexadecafluoro Phthalocyanine |
| MPc | Metal Phthalocyanine |
| UV | ultraviolet |
| VIS | visible |
| $E_g$ | Energy band gap |
| XRD | X-ray Diffraction |
| AFM | Atomic Force Microscopy |
| OSC | Organic Semiconductor |
| OLED | Organic light-emitting diode |
| Pc | Phthalocyanine |
| Co | Cobalt |
| Mn | Manganese |
| CuPc | Copper phthalocyanine |
| RMS | Roughness Mean Square |
| PVD | Physical vapor deposition |
| IR | Infrared |
| FWHM | Full Width at Half Maximum |

## TABLE OF CONTENTS

# CHAPTER 1

# INTRODUCTION

## 1.1 General Introduction

Inorganic semiconductor materials, such as silicon, are commonly used and integrated into an electronic industry for a long time. However, due to their complex process and high cost, the application of the silicon based has been strictly limited (Lü et al., 2007). Organic semiconductors (OSCs) are gaining popularity owing to their appealing qualities that set them apart from their usual inorganic silicon-based counterparts; lightweight, low-cost manufacture, low-temperature processing, flexibility, and environmentally-friendly application (Köhler & Bässler, 2015). OSCs are compounds that mainly consists of carbon and hydrogen. The recent commercialization of organic light-emitting diodes (OLEDs) for smartphones proved that organic compounds have exciting applications in various other electric and optoelectronic devices (Köhler & Bässler, 2015; Reineke et al., 2009). For example, solar cells, transistors, photodetectors, and lasers may be made with OSCs efficiently (Kietzke, 2007; Kuehne & Gather, 2016; H. Ren et al., 2021; Zschieschang & Klauk, 2019).

In recent years, phthalocyanines (Pcs) have piqued the interest of many researchers due to their properties (Nyokong, 2011). Pcs are aromatic macrocyclic compound with an intense blue-green hue and commonly used in dyeing (Van Staden, 2015). The structure of Pcs consists of 16-membered rings with presence of alternating carbon and nitrogen (Wang et al., 2012). The name of phthalocyanine is derived from the Greek words

'naptha', which means rock oil, while 'cyanine' means dark blue (Van Staden, 2015). Sir Reginald Linstead used it to characterize the class of this compound for the first time in 1934 (Van Staden, 2015). Pc is valuable for its ability to pass electrons and has similar derivatives to porphyrin (Sakamoto & Ohno-Okumura, 2009b). Pc molecules are also highly stable organic semiconductors (J. Ren et al., 2011). Due to their properties, Pcs are extremely useful in a wide variety of innovative and evolving high-tech applications as organic semiconductors, leading to the application of organic photovoltaic cells, organic light-emitting diodes (OLEDs), and gas sensors (Collins & Mohammed, 1986; Karan & Mallik, 2007; Kippelen & Brédas, 2009; Sakamoto & Ohno-Okumura, 2009b; Van Staden, 2015).

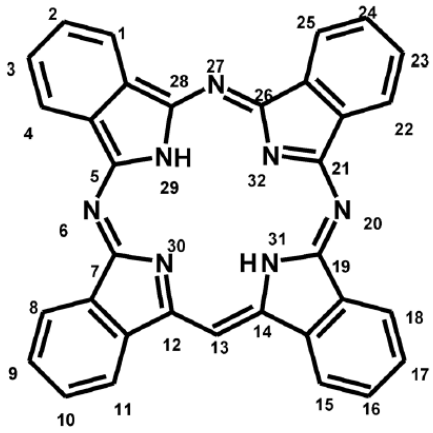


**Figure 1.1:** The structure of phthalocyanine (Nyokong, 2011).

The molecular core of Pcs could also host a metal ion, M (Wang et al., 2012). Metallopthalocyanines (MPcs) are planar organic molecules, and cobalt (Co) and manganese (Mn) are some of the elements which are commonly used as the metal ion M (El-Nahass et al., 2003; Sridevi et al., 2021). The utilization of MPcs as organic semiconductors material is an added advantage since they could potentially carry charges

and improve properties (Witte & Wöll, 2004). Therefore, many MPcs have been studied to synthesize and characterize their properties and application. MPcs have monoclinic crystalline arrangement with a herringbone-type packing of a molecule (Witte & Wöll, 2004). Using different metal ions produces different changes to the structure; the same goes with copper hexadecafluoro phthalocyanine ($F_{16}$CuPc). This fluorinated copper phthalocyanine is an n-type semiconductor and works well as an electron acceptor (J. Ren et al., 2011).

The preparation of $F_{16}$CuPc thin films is carried out by using the thermal evaporation method. The $F_{16}$CuPc thin films are characterized to study the optical, structural, and morphological properties.

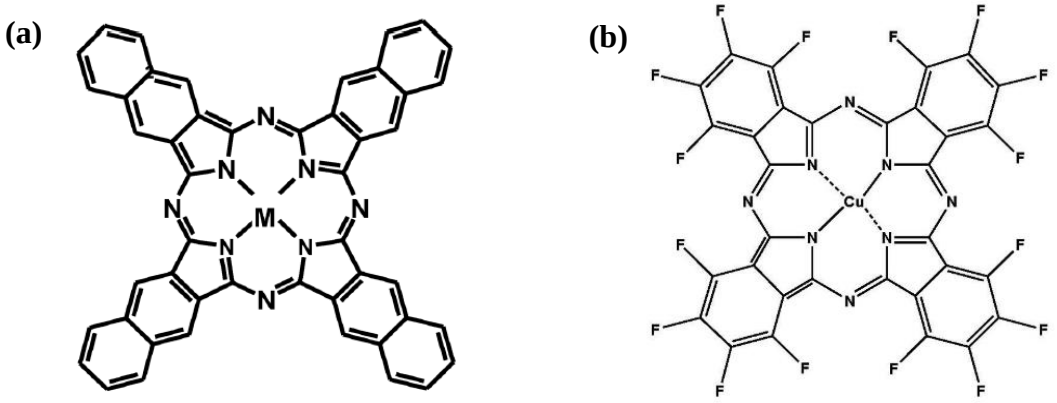


**Figure 1.2: (a)** The structure of metallophthalocyanine (Nyokong, 2011), **(b)** The structure of copper hexadecafluoro phthalocyanine (Zhang et al., 2019).

## 1.2 Problem Statement

An inorganic compound such as silicon has long been applied to microelectronic devices. Despite their widespread use, the inorganic compound has some drawbacks, including being costly, brittle, and complex (Çavuş et al., 2013). The presence of organic compounds has given a new perspective of its use in research and technology to overcome the problem. Organic compounds have unique characteristics and properties such as high absorption coefficient, optical selectivity, low weight, flexibility, and electronics tuneability, making them ideal for the use of fabricating microelectronic devices (Çavuş et al., 2013; Basir et al., 2021). Due to its properties, Pcs is becoming one of the most studied organic compounds.

However, there is lacking in scientific literature on application of $F_{16}$CuPc material as a high potential organic compound. Therefore, this study is interested in determining the optical, structural, and morphological properties of $F_{16}$CuPc. This study might be helpful for other researchers who are planning to use $F_{16}$CuPc as a material in the fabrication and application of organic semiconductors.

## 1.3 Research Objectives

The present study is aimed to provide a comprehensive investigation on the optoelectronic parameters of $F_{16}CuPc$ in order to reveal its potential application for optoelectronic devices. Hence, in this work, the $F_{16}CuPc$ thin film have been thermally deposited and the temperature of post-annealing have been varied. The novelty of this work is to quantify the optical parameters such as optical absorption, dielectric constant, refractive index, and optical conductivity of $F_{16}CuPc$ as well as to investigate the variations of structural and morphological properties of $F_{16}CuPc$ by varying annealing temperatures. Three objectives have been laid out:

i. To determine the optical parameters of $F_{16}CuPc$.

ii. To investigate the structural properties of $F_{16}CuPc$ by varying the annealing temperature.

iii. To investigate the morphological properties of $F_{16}CuPc$ by varying the annealing temperature.

# CHAPTER 2

# LITERATURE REVIEW

## 2.1 Introduction

Chapter 2 consists of a review of the study of $F_{16}CuPc$. This chapter will review the history of organic semiconductors and phthalocyanine. Also, the optical properties of $F_{16}CuPc$, which uses UV-Vis spectrometer, the structural properties of $F_{16}CuPc$, analyzed by an X-ray diffractometer (XRD) spectrometer, and the morphological properties using Atomic Force Microscopy (AFM) from the previous researchers are discussed.

## 2.2 Organic Semiconductors

Henry Letheby created a partially conductive substance by anodizing aniline in sulfuric acid in 1862, and the substance was polyaniline (Rasmussen, 2017). In the 1950s, polycyclic aromatic compounds created semiconducting charge-transfer complex salts with halogens (Mehta et al., 1957). Later, it was found that organic semiconductors are insulators but become semiconductors when the electrode injected charge carriers (Kallmann & Pope, 1960). They discovered that a hole current might flow through an anthracene crystal when it is in contact with an electrolyte with positively biased containing iodine, which acts as a hole injector. The earlier result inspired this research that aromatic hydrocarbons become conductive when it is mixed with molecular iodine due to the formation of a charge-transfer complex (Akamatu et al., 1956).

The critical parameter controlling injection is then replaced with semiconducting material. In 1977, excellent conductivity in oxidized and iodine-doped polyacetylene was discovered by Hideki Shirakawa et al. (1977) which then were awarded the Nobel Prize in Chemistry in 2000 for "invention and development of conductive polymers.

## 2.3 Phthalocyanine

According to Thomas (1990), phthalocyanine is derived from the Greek term for naphtha (rock oil) and cyanine (dark blue). Professor Reginald P. Linstead first used "phthalocyanine" to describe a class of organic compounds containing metal-free phthalocyanine, metal phthalocyanine, and their derivatives. In 1907, at the South Metropolitan Gas Company in London, Braun and Tcherniac found a blue substance after heating o-dibromobenzene with cuprous cyanide, and this substance probably was phthalocyanine. In 1927, de Diesbach and von der Weid attempted to make nitriles of benzene by reacting o-dibromobenzene with cuprous cyanide and obtained copper phthalocyanine as the product.

Also at the beginning of 1929, Professor Linstead and his students were supported by grants from Imperial Chemical Industries, in a series of investigations determined the structure of phthalocyanine molecule and announced this achievement in 1933 and 1934. X-ray studies of phthalocyanine and its metal derivatives including nickel and copper demonstrated that phthalocyanine, nickel, and copper phthalocyanines form monoclinic crystals. The entire molecule lies in one plane, with the possible exception of the two central hydrogen atoms.

## 2.4 Copper Hexadecafluoro Phthalocyanine

### 2.4.1 Optical Properties

In 2007, a study on $F_{16}$CuPc as an electron acceptor material is conducted to fabricate organic photovoltaic cells. According to Jiang et al. (2007), $F_{16}$CuPc and *para*-sexiphenyl (p-6P) are used and purified twice by thermal gradient sublimation. The layers of *para*-sexiphenyl (p-6P) and F16CuPc have evaporated on PEDOT:PSS/ITO substrate in the vacuum of $10^{-4}$ – $10^{-5}$ Pa at a rate of about 1 nm/min. Then, a 40 nm Au electrode was deposited on the active organic layers by thermal evaporation at $10^{-4}$ Pa, defining an active area of 0.12 $cm^2$. From the graph of absorbance, $F_{16}$CuPc shows three absorption peaks at around 653, 701, and 780 nm in the visible (Vis) region.

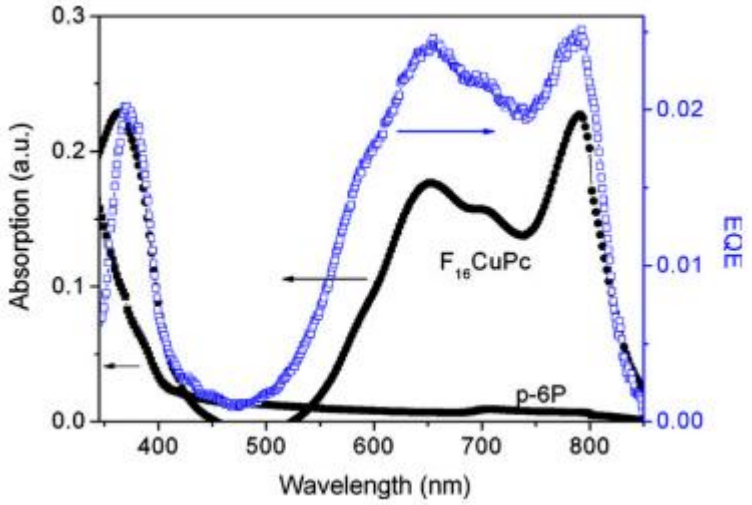


**Figure 2.1:** The absorbance of $F_{16}$CuPc in fabricating organic photovoltaic cells (Jiang et al., 2007).

A study on $F_{16}$CuPc thin films was done using vacuum annealing in 2012. According to Koshy and Menon (2012), the deposition rate is controlled at $10^{-12}$ nm/min,

and the glass substrates are placed at a distance of 11 cm from the source. The $F_{16}CuPc$ thin films are annealed in a vacuum for 1 h at 100 ℃, 150 ℃, and 200 ℃, and a few parameters of optical properties are observed. The absorbance of $F_{16}CuPc$ thin films shows a peak at 358 nm, which is in the ultraviolet (UV) region. Also, there are two peaks at 638 nm and 792 nm in the visible (Vis) region. They also report it the optical band gap energy ($E_g$) for $F_{16}CuPc$ thin films is $(3.06 \pm 0.01)$ eV.

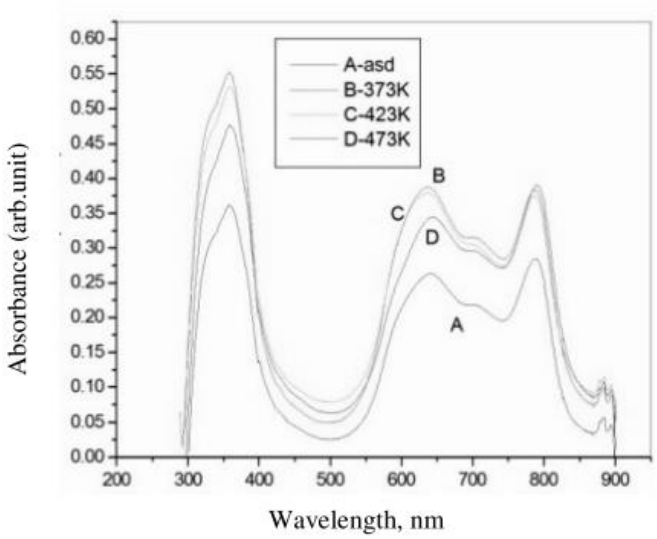


**Figure 2.2:** The absorbance of $F_{16}CuPc$ thin films with different annealing temperature (Koshy & Menon, 2012).

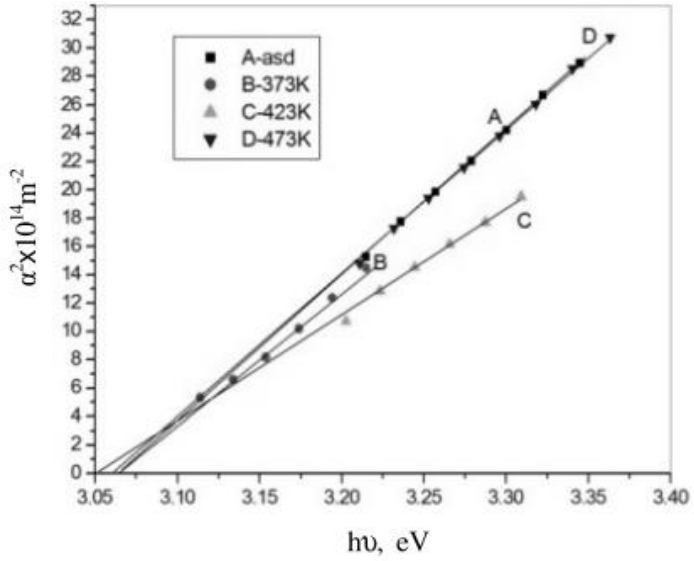


**Figure 2.3:** The graph of $\alpha^2$ versus the energy of $F_{16}CuPc$ thin films to find the band gap (Koshy & Menon, 2012).

### 2.4.2 Structural Properties

A study on ambipolar organic thin-film transistors based on $F_{16}$CuPc and copper phthalocyanine (CuPc) is done. The $F_{16}$CuPc thin film is continually vacuum-deposited, and the substrate temperature is set to 120 °C. According to Rongbin et al. (2005), the $F_{16}$CuPc thin film has spacing, *d* of 1.42 nm with (2 0 0) orientation.

In 2006, a study on the correlation of morphology and electronic properties of $F_{16}$CuPc thin films was done. The $F_{16}$CuPc thin films are deposited with different substrate temperatures such as 75 °C, 100 °C, 125 °C, and 150 °C. According to Ye et al. (2006), $F_{16}$CuPc thin films have spacing, d of 1.43 nm with (2 0 0) orientation. It is also stated that increasing substrate temperature improves the molecular structure, thus enhancing crystallinity.

A study on $F_{16}$CuPc thin films was conducted to compare their structural properties with the effect of annealing. The $F_{16}$CuPc thin films are deposited by using vacuum annealing. According to Ye et al. (2010), the spacing d observed is 1.44 nm with (2 0 0) orientation.

### 2.4.3 Morphological Properties

In the same study, Ye et al. (2006) has reported that elongated bent strips are seen on the surface of $F_{16}CuPc$ thin films which the substrates are annealed at 75 °C, 100 °C, 125 °C, and 150 °C. They observed the topographic of $F_{16}CuPc$ thin films with an area of $2\mu m \times 2\mu m$ by using Atomic Force Microscopy (AFM). The results show that the length of the strips was increasing as the temperature of substrates increased. The Roughness Mean Square (RMS) value increases as well.

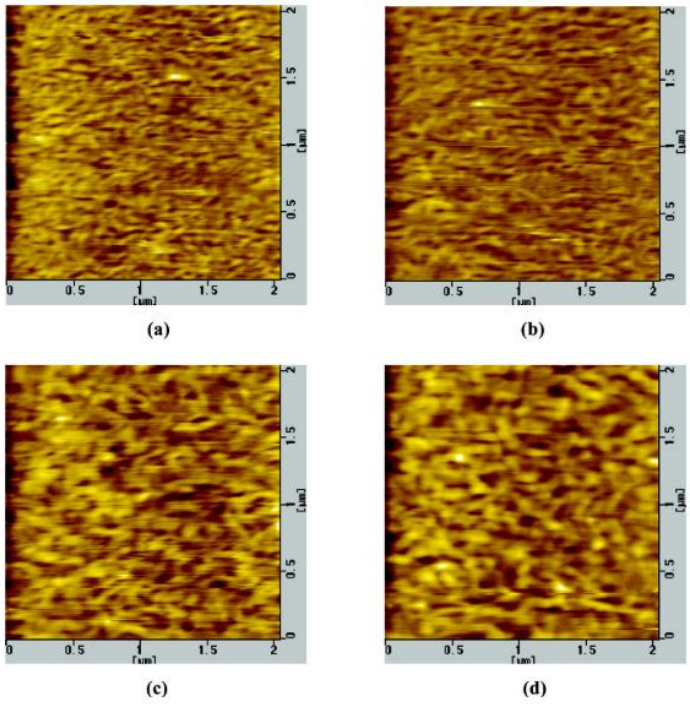


**Figure 2.4:** AFM images of $F_{16}CuPc$ thin films with a substrate temperature of **(a)** 75 °C, **(b)** 100 °C, **(c)** 125 °C and **(d)** 150 °C (Ye et al., 2006).

In 2008, Ye et al. (2008) conducted a study to observe the structure and morphological of $F_{16}CuPc$ and CuPc heterojunction using vacuum deposition, and the

substrate temperature is set at 120 °C. By using AFM on $F_{16}$CuPc thin films, elongated bent strips could be seen on the surface of the substrates.

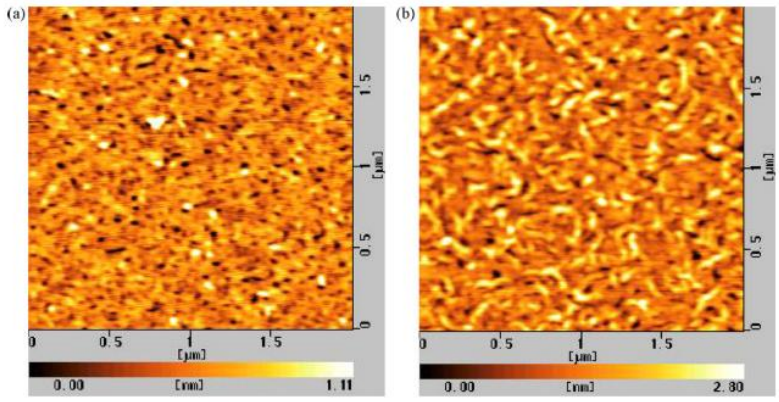


**Figure 2.5:** AFM images of $F_{16}$CuPc thin films with a thickness of **(a)** 5 nm and **(b)** 10 nm (Ye et al., 2008).

In 2012, a study on morphological properties was done to reduce grain boundaries and contact resistance in $F_{16}$CuPc thin films. The deposition rate is set as low as possible (~0.1 Å/s), which is stated to reduce the structural disorder and substrate temperature of 40 °C and 100 °C with $F_{16}$CuPc thin film thickness of 65 nm. (Yadav et al., 2012). According to the researchers, $F_{16}$CuPc thin films with a temperature substrate of 40 °C consist of isotropic grains. The morphology also shows a polycrystalline image with the grain size of 40 nm to 60 nm, while $F_{16}$CuPc thin films with a temperature substrate of 100 °C consist of elongated rod-like structures. Another $F_{16}$CuPc thin film with substrate temperature of 100 °C is then deposited using a higher deposition rate of 10 Å/s and shows that the elongation of the rod-like structure is much weaker.

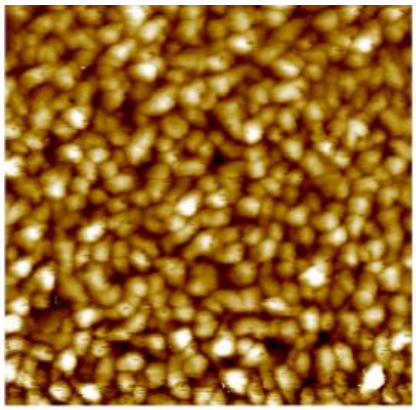

**Figure 2.6:** AFM image of $F_{16}CuPc$ thin film with a substrate temperature of 40 °C (Yadav et al., 2012).

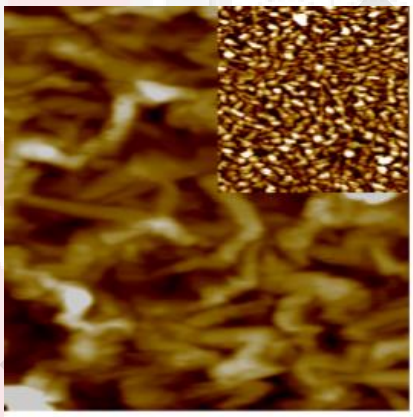

**Figure 2.7:** AFM image of $F_{16}CuPc$ thin film with a substrate temperature of 100 °C. The inset of the figure shows the AFM image of $F_{16}CuPc$ thin film with a substrate temperature of 100 °C with a deposition rate of 10 Å/s (Yadav et al., 2012).

# CHAPTER 3

# METHODOLOGY

## 3.1 Introduction

This chapter depicts the procedure for the preparation and characterization of $F_{16}CuPc$ thin films. In this experiment, $F_{16}CuPc$ thin films were prepared via thermal evaporation. Thermal evaporation is a physical vapor deposition (PVD) method that includes material evaporation in a vacuum environment to form a thin film. The $F_{16}CuPc$ thin films were formed by placing $F_{16}CuPc$ powder in a tungsten boat with a deposition time of 60 seconds. Then, the $F_{16}CuPc$ thin films were annealed for 30 minutes with varying temperatures (50 °C, 100 °C, and 200 °C). The optical properties of $F_{16}CuPc$ thin films were studied by using UV-Vis-NIR spectroscopy (UV-VIS-NIR), the structural properties were identified by X-ray diffraction (XRD), while the morphological properties were observed by Atomic Force Microscopy (AFM). The process for preparing $F_{16}CuPc$ thin films is shown in Figure 3.1.

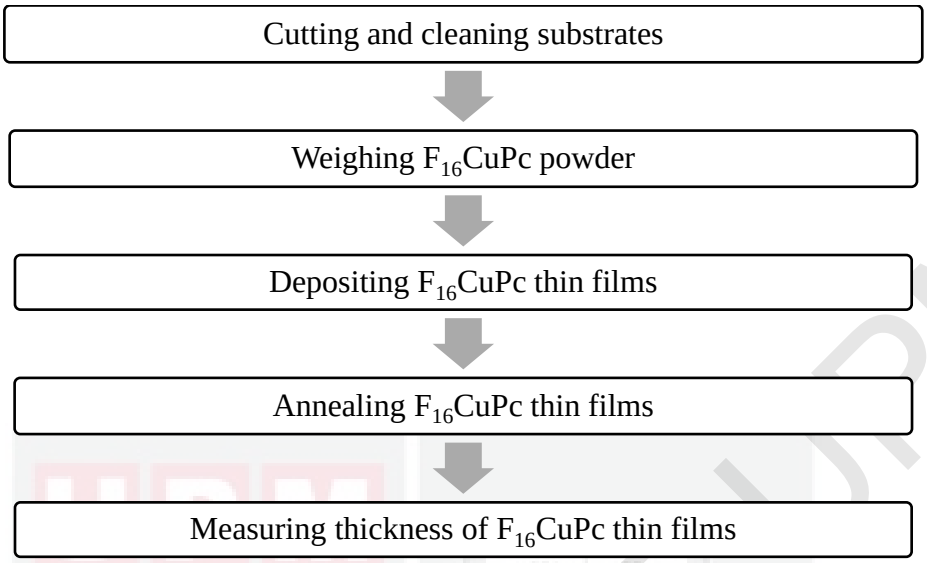


**Figure 3.1:** Flow chart for forming $F_{16}$CuPc thin films.

### 3.2 Reagents and Materials

The organic material, $F_{16}$CuPc, was bought from Sigma Aldrich (St. Louis, MO, USA) and used without further purification. Glass cover slides 76 × 26 mm with thickness between 1.0 - 1.2 mm were purchased from Menzel-Glaser.

### 3.3 Preparation of Substrates

Before the deposition process, the glass slides were cut using a glass cutter into 15 × 20 mm sizes to be used as substrates. The substrates were put in a beaker, and ethanol was poured into the beaker until the glass substrates were covered. The beaker was then inserted into an ultrasonic cleaner filled with deionized water to clean the glass substrates from dirt and fingerprints. The ultrasonic cleaner was switched on for 10 minutes. After 10 minutes, the ethanol was poured out, and the glass substrates were washed with deionized water. The steps were repeated two times by replacing ethanol with isopropanol and acetone. The substrates were then dried.

**Figure 3.2:** The glass substrates were sonically cleaned by ultrasonic cleaner for 10 mins.

### 3.4 Weighing the Material

15 mg of $F_{16}$CuPc powder was weighed by using an electronic balance.

### 3.5 Deposition of Thin Films

The deposition of $F_{16}$CuPc thin films was performed using a thermal evaporator of type Edwards Auto 306. The chamber pressure was waited for around 2 hours and ensured to be $1.0 - 1.1 \times 10^{-5}$ MB. In the meantime, the components of the thermal evaporator, including the bell jar, were cleaned before being used with acetone to avoid contamination during the deposition process. The bell jar is greased with vacuum grease of Dow Corning High Vacuum Grease was used as it helps in sealing joints in vacuum systems. Next, a tungsten boat was placed, and 15 mg of $F_{16}$CuPc powder was poured into it to be evaporated. The suitable substrate holder was put, and the glass substrates were placed onto it.

The thermal deposition process was done after the chamber pressure was ensured to be $1.0 - 1.1 \times 10^{-5}$ MB. The power supply was made sure to be pre-set at 10 (A), and the rotary knob was at the value of "0". The power supply was switched on from "0" to "LT" and the knob was slowly turned to value "4", and the indicated current was 38 A. The shutter was in the "open" position for the deposition for 60 s, and then the shutter was closed after the deposition process was done. The knob was turned back slowly to the value of "0", and the power supply was switched off.The machine's switch was turned off before The bell jar was handled with care and cleaned with acetone. The samples were taken out, and the water tap was turned off after 1 hour for cooling purposes.


**Figure 3.3:** Edward Auto 306 thermal evaporator.

**Figure 3.4:** The tungsten boat was placed for the thermal deposition process.

**Figure 3.5:** The glass substrates were placed on the substrates holder.

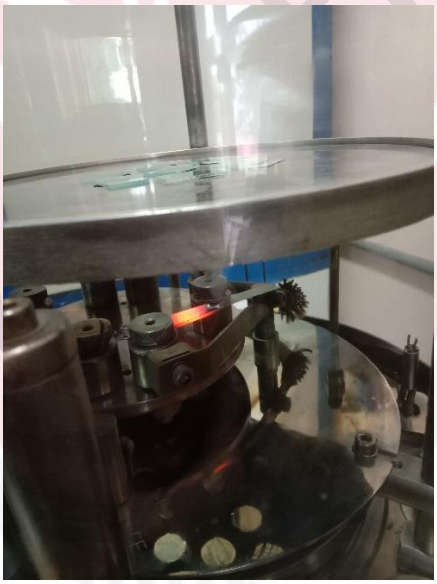

**Figure 3.6:** The tungsten boat filled with 15 mg of $F_{16}CuPc$ powder was heated up.

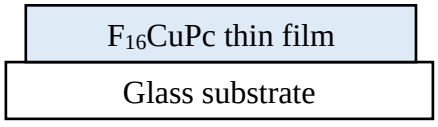


**Figure 3.7:** The structure schematic drawing of $F_{16}CuPc$ thin film.

### 3.6 Annealing

Thermal annealing is the process of heating a sample at a specific temperature, maintaining it at a temperature for a particular duration, and cooling down the sample to room temperature at a particular rate. The $F_{16}CuPc$ thin films were annealed for 30 mins with a varied temperature of 50 °C, 100 °C, and 200 °C on a hot plate.


**Figure 3.8:** As-deposited and annealed $F_{16}CuPc$ thin films.

### 3.7 Sample Characterization

After the thermal deposition process, the thickness of $F_{16}CuPc$ thin films was measured using a surface profilometer. The samples were also characterized using UV-Vis-NIR spectroscopy, X-ray Diffraction (XRD), and Atomic Force Microscopy (AFM) to study the optical, structural, and morphological properties.

#### 3.7.1 Profilometer

Profilometer of type DEKTAK 8000 KLA Tencor P-6 was used to measure the thickness of F16CuPc thin films at Low Dimensional Material Research Center (LDMRC), Physics Department, Faculty of Science, Universiti Malaya. The profilometer includes the mechanical and optical components for sample placement, sample viewing, scanning, and measurement.

The sample was put on the sample stage, and the stylus was positioned for scanning with the help of controls for X-Y movement, rotation, and leveling. The sample was placed using the trackball. In fine positioning mode, a crosshair reference appears on the monitor. This software reticle superimposes over the video image of the sample surface. A wafer or disk-shaped template appears on the monitor in the coarse positioning mode. The desired location is pointed on the template, and double-click the location. The gantry would automatically convert to that position.

When the scanning process was performed, the stylus was lowered and contacts the sample surface. The stage moves the sample as the stylus moves over the sample's surface. The visual monitor shows the actual scanning of the sample and the graphing of

the results. The stylus would automatically retract after the scanning process is done. Figure 3.9 shows the image of surface profiler used in this work.

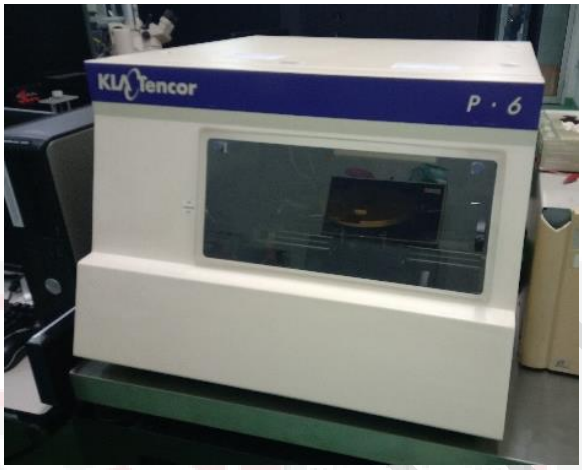


**Figure 3.9:** The surface profiler that was used to measure the thickness of $F_{16}CuPc$ thin films.

### 3.7.2 Ultraviolet Visible Near-Infrared (UV-Vis-NIR) spectroscopy

UV-Vis-NIR spectroscopy of type PERKIN-ELMER LAMBDA 750 was used to observe the optical properties of $F_{16}CuPc$ thin films at Low Dimensional Material Research Center (LDMRC), Physics Department, Faculty of Science, Universiti Malaya. Optical properties of $F_{16}CuPc$ thin films such as absorbance were observed from the characterization and then compared to the reported. The wavelength used ranges from 200-900 nm.

The $F_{16}CuPc$ thin film and clean glass substrate reference were placed at the sample and reference holders. Deuterium and tungsten halogen are used as light sources, and it passes through a few components such as double holographic grating monochromators, beam mask, beam depolarizer, chopper. Double holographic grating monochromators are for ultra-low stray light performance, high accuracy, and high

reproducibility. Beam mask allows precise adjustment of the beam height to match samples of different dimensions. Beam depolarizer is used to corrects for inherent instrument polarization to allow accurate measurements of birefringent samples. The chopper switches between sample and reference beam. They provide individual blank readings for a sample and reference and increasing measurement accuracy.

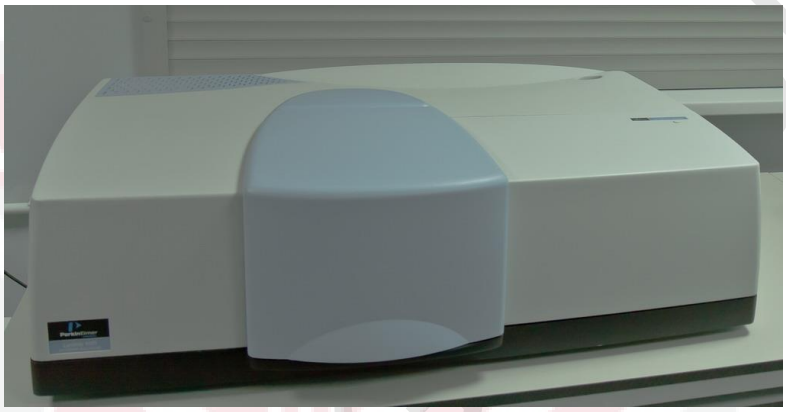

**Figure 3.10:** The UV-Vis-NIR spectrometer used to measure the absorbance of $F_{16}CuPc$ thin films.

### 3.7.3 X-ray Diffraction (XRD)

The XRD is a method used to obtain the structure of materials based on their diffraction pattern. In addition to phase identification. A diffraction pattern could be obtained by scattering angles, forming constructive interferences of X-rays. XRD of type PANalytical – Philips, PW3040/60 was used at Department of Physics, Faculty of Science, Universiti Putra Malaysia to determine the structural properties of $F_{16}CuPc$ thin films.

The essential components of an X-ray diffractometer are an X-ray tube, a sample holder, and an X-ray detector. In a cathode ray tube, the X-rays are generated to produce accelerated electrons aimed toward a target. Due to random orientation when scanning the sample with an angle, constructive interference occurs, resulting in increased intensity and satisfying Bragg's Law.

$$2d \sin\theta = n\lambda \quad (1)$$

Here $d$ is the inter-planar distance between the planes in the atomic lattice, $\theta$ is the incidence angle, $n$ is the integer, and $\lambda$ is the wavelength of the X-rays. The exact directions emerge as reflections on the diffraction pattern.

**Figure 3.11:** The XRD spectrometer used to identify the structural properties of $F_{16}CuPc$ thin films.

### 3.7.4 Atomic Force Microscopy (AFM)

**Surface Sensing**

An AFM of type Dimension Edge (Bruker) was used to analyse the morphological properties of $F_{16}CuPc$ thin films at Department of Physics, Faculty of Science, Universiti Putra Malaysia. An AFM uses a cantilever with a sharp tip to scan over a sample surface as the tip approaches the surface. The attractive close-range forces between the surface and the tip cause the cantilever to bend towards the surface. As the cantilever is brought even closer to the surface, the increasingly repulsive force causes the cantilever to bend away from the surface.

**Detection Method**

An AFM has a Z-scanner that moves the cantilever up and down, an XY-scanner that moves the sample back and forth underneath the cantilever, and a position detector that records the bending of the cantilever. The position sensor works by tracking a laser beam reflected off the flat top of the cantilever. Any bending in the cantilever will cause changes in the direction of the beam. The position detector then tracks and records those beam changes.

**Imaging**

Using the detection method, an AFM images the topography of a sample surface by scanning the cantilever over a region of interest. The raised and lowered features on the sample surface influence the bending of the cantilever measured by the position detector. AFM generates an accurate topographic map of the surface by using a feedback loop to control the height of the tip above the surface.

**Figure 3.12:** AFM spectrometer used to observe the morphological properties of $F_{16}CuPc$ thin films.

# CHAPTER 4

# RESULTS AND DISCUSSION

## 4.1 Introduction

Chapter 4 will discuss and review the results obtained from the methodology that has been done in Chapter 3. The optical parameters of $F_{16}CuPc$ thin film were determined using a UV-Vis spectrometer. The structural properties were analysed using the X-ray Diffraction (XRD), and the morphological properties of $F_{16}CuPc$ thin film were studied using an AFM spectrometer.

## 4.2 Optical Parameters of $F_{16}CuPc$ thin films

Prior the optical characterizations, the thickness of thin films were measured by using a surface profilometer. For each sample, the measurements were repeated at three different locations on the thin films surface, then the average of the measurements were calculated. The measured thickness was tabulated in Table 1. The as-deposited $F_{16}CuPc$ thin film exhibits the highest thickness compared to the other thin films, which were annealed at different temperature (50 °C, 100 °C and 200 °C) in ambient condition. The thickness decreases as the organic films were annealed to a higher temperature. This may be due to the oxidation of the thin films, as the annealing process were carried out in ambient conditition. It is also worth noting that, the thickness of thin films which were annealed at 50 °C and 100 °C were inconsistent as this might due to the non-uniform film

formation during deposition process. It was found that the standard deviation of the measured thickness is about 1-5%, which is an acceptable error in nanoscale measurements.

**Table 1:** Measured thickness of $F_{16}CuPc$ thin films

| Sample | Measured thickness (nm) | | | Average thickness (nm) | Standard deviation |
|---|---|---|---|---|---|
| As-deposited | 41.03 | 45.16 | 41.17 | 42.45 | 2.41 |
| 50 °C | 31.12 | 36.75 | 33.45 | 33.77 | 2.98 |
| 100 °C | 34.67 | 39.22 | 30.49 | 34.79 | 4.47 |
| 200 °C | 28.07 | 29.15 | 28.67 | 28.63 | 0.94 |

The optical absorption spectra of all the prepared samples of $F_{16}CuPc$ in the wavelength of 300 to 900 nm were recorded. The absorption spectra of as-deposited and annealed $F_{16}CuPc$ thin films are shown in Figure 4.1. It is found that there is insignificant effect of absorbance spectra on temperature variations for $F_{16}CuPc$ thin film. The light that passes through a surface will eventually be absorbed, transmitted, and reflected. Absorbance is neither reflected nor transmitted; the light goes into the material but never comes out. When the material absorbs light, it takes the energy of the light and changes it into another form of energy, such as heat.

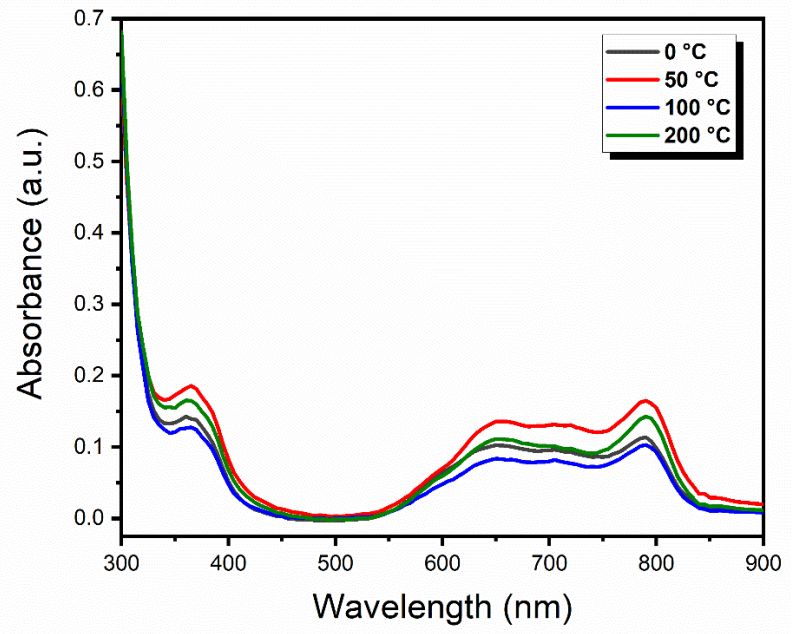


**Figure 4.1:** The absorbance spectra of $F_{16}CuPc$ thin films.

From Figure 4.1, one can notice that the absorption spectra consists of two bands: B band (Soret band) and Q band. According to Koshy & Menon (2012), the molecular spectra in Pc's are derived from the aromatic 18 $\pi$ electron system's molecular orbitals and the overlapped orbital on the central metal atom. From the result, it is observed that as-deposited and annealed $F_{16}CuPc$ thin films are performing well in absorbing light in the ultraviolet (UV) range, 200 nm to 400 nm. peaking at 360 nm. In the meantime, a broad peak is observed in the visible range (Vis), 400 nm to 800 nm, which is called the Q band. The Q band split up into two peaks positioned at 650 nm and 789 nm due to the allowed $\pi$-$\pi^*$ orbitals (Sakamoto & Ohno-Okumura, 2009a). When two double bonds are conjugated, one of the bonding orbitals is raised in energy and the other lowered relative to the energy of an isolated double bond. The same applies to the antibonding orbitals and as a result, the transition probability is enhanced, the wavelength of maximum

absorption moves to a longer wavelength, and the intensity of absorption is frequently increased (Sakamoto & Ohno-Okumura, 2009a).

The relation between transmittance and absorbance can be proven with Beer's Law. According to Beer's Law,

$$A = log_{10} \frac{I_0}{I} \quad (2)$$

Where,

$I_0$ = intensity of light

$I$ = intensity of light that passes through the surface

The transmittance can be defined as a part of the light passing through the opposite side of a surface. The absorbance can be related to the transmittance. Transmittance can also be referred to as the ratio of the intensity of light ($I_0$) to the quantity of intensity that passes through the surface ($I$).

$$T = \frac{I}{I_0} \quad (3)$$

By substituting equation (3) into (2) and taking the logarithm, one can obtain a formula of transmittance of light:

$$T = 10^{-A} \quad (4)$$

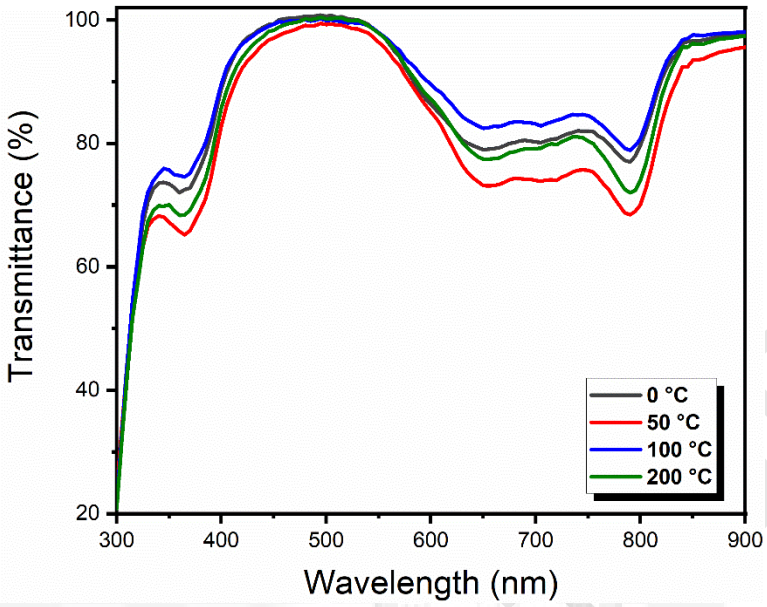


**Figure 4.2:** The transmittance of $F_{16}$CuPc thin films.

Figure 4.2 shows the transmittance of $F_{16}$CuPc thin films. From the graph, the transmittance percentage sharply increases at the earlier Vis region with a shoulder at 345 nm. It remains constant to almost 550 nm, with the maximum transmittance percentage at 495 nm before plummeting to around 650 nm. The graph also shows a sharp decline to 790 nm before sores to almost maximum in the infrared (IR) region. This means that $F_{16}$CuPc thin films allow more lights to pass through around 400 nm to 550 nm and 800 nm to 900 nm. The transmittance percentage decreases show that within 300 nm to 400 nm and 600 nm to 800 nm, $F_{16}$CuPc thin films absorb more light due to strong photo absorption in this wavelength range.

Reflectance is defined as the amount of light reflected from the surface and can be related to absorbance and transmittance (El-Nahass et al., 2004). The value of reflectance is deduced from the absorbance data as the following:

$$R = 1 - (A + T) \tag{5}$$

Where,

A = absorbance

T = transmittance

R = reflectance

Figure 4.3 depicts the reflectance spectra of $F_{16}CuPc$ thin films. It is obviously shown that, there are two broad peaks from 600 nm to 800 nm. The reflectance percentage fluctuates in the earlier UV region and forms a shoulder at 360 nm. The spectra then plunge from 400 nm to almost minimum at 500 nm before soaring up and forming two broad peaks at 650 nm and 790 nm. The reflectance spectra then decrease sharply to almost 850 nm. This means that the light is reflected mainly in the wavelength range of 300 nm to 400 nm and 600 nm to 800 nm.

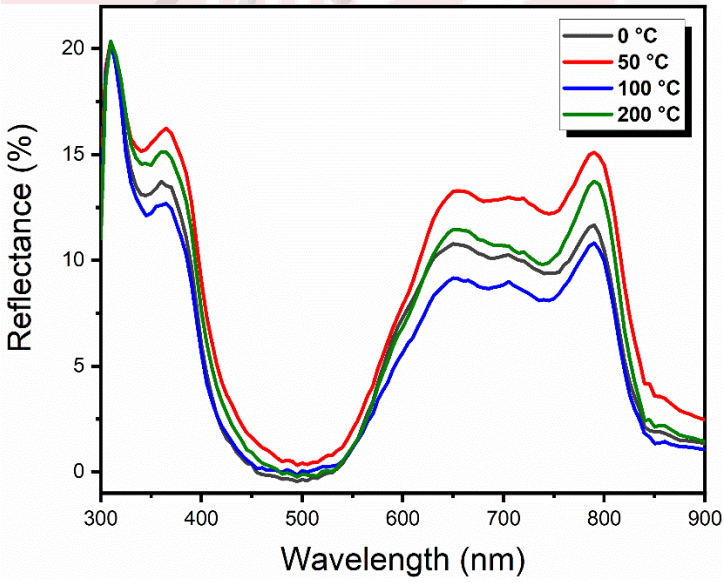


**Figure 4.3:** The reflectance of $F_{16}CuPc$ thin films.

The absorption coefficient describes how much the material of a given thickness absorbs light of a given color. The absorption coefficient for this study is denoted by $\alpha$ and was obtained by using this formula:

$$\alpha = \frac{2.303 \times A}{d} \quad (6)$$

Where,

$\alpha$ = absorption coefficient

A = absorbance

$d$ = thickness of the film

Figure 4.4 shows the absorption coefficient of $F_{16}CuPc$ thin films versus wavelength. The absorption coefficient of the $F_{16}CuPc$ thin films has a high value in the order of $10^5$ $cm^{-1}$, which might be suitable for applying light-sensing as it has assertive absorption behavior. The organic thin films have a significant absorption coefficient with two broad peaks at 645 nm and 789 nm, and it also presents a peak at 360 nm in the earlier part of the Vis region. We can relate Figure 4.4 and Figure 4.5 together. The absorption coefficient is low as photon energy is less than the bandgap value (refer Figure 4.8), while the absorption coefficient rapidly increases when the photon energy is more significant than the band gap value. From Figure 4.5, we can see that the absorption coefficient is relatively strong, around 1.50 eV to 1.90 eV and from 3.15 eV to 4.20 eV.

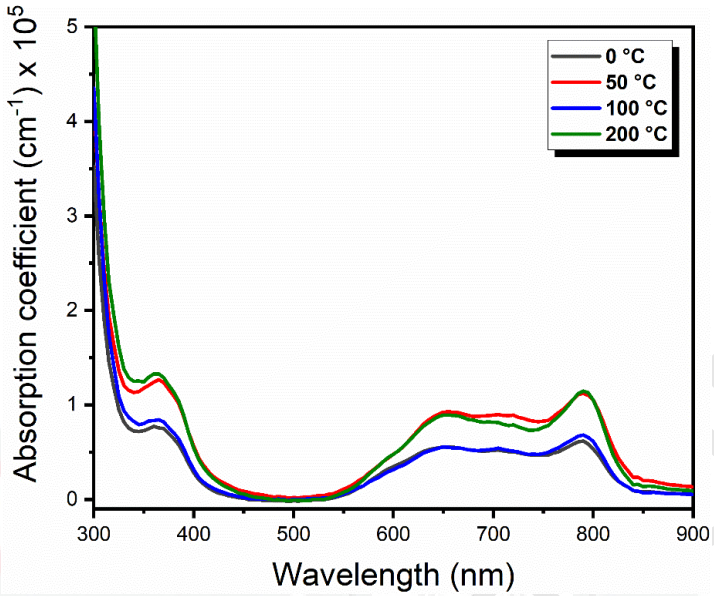


**Figure 4.4:** The absorption coefficient of $F_{16}CuPc$ thin films versus wavelength.

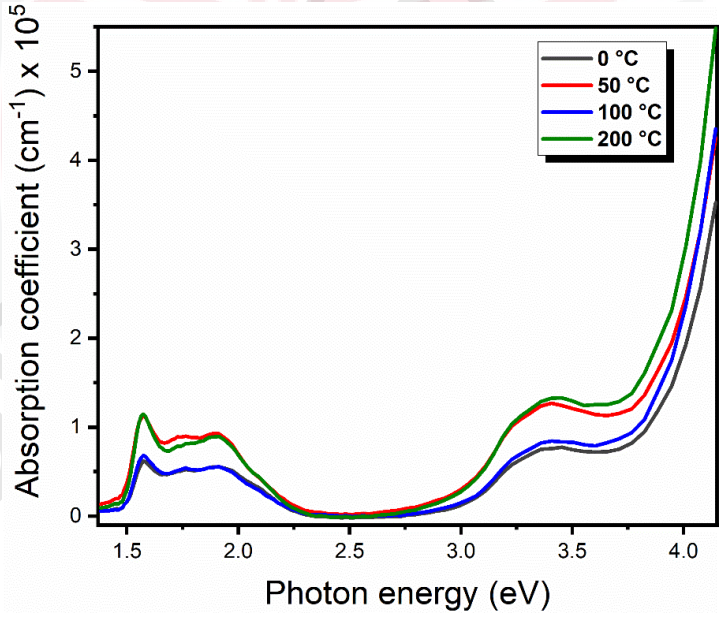


**Figure 4.5:** The absorption coefficient of $F_{16}CuPc$ thin films versus energy.

The extinction coefficient is defined as the energy loss of light spectrum within $F_{16}CuPc$ thin films. It can also be defined as a fraction of transmitted light and absorption

per unit distance of the penetration medium (Köhler & Bässler, 2015). It is a material characteristic under a precisely defined set of conditions, such as wavelength and temperature. The extinction coefficient value can be obtained by using the formula $n^* = n + ik$, which is related to the refractive index. According to Koshy & Menon (2012), the value of *k* can be calculated by the formula:

$$k = \frac{\alpha\lambda}{4\pi} \tag{7}$$

Where,

k = extinction coefficient

$\alpha$ = absorption coefficient of the film

λ = wavelength

Figure 4.6 displays the extinction coefficient on the wavelength for $F_{16}$CuPc thin films. As seen from the figure, we can see that the extinction coefficient of $F_{16}$CuPc thin films is relatively high in the range of 645 nm to 800 nm. The highest peak is at 792 nm, with a wide shoulder at 645 nm. There is also a peak in the UV region at 368 nm. The $F_{16}$CuPc thin films presented a high extinction coefficient in the Vis region, making them suitable for light sensing application.

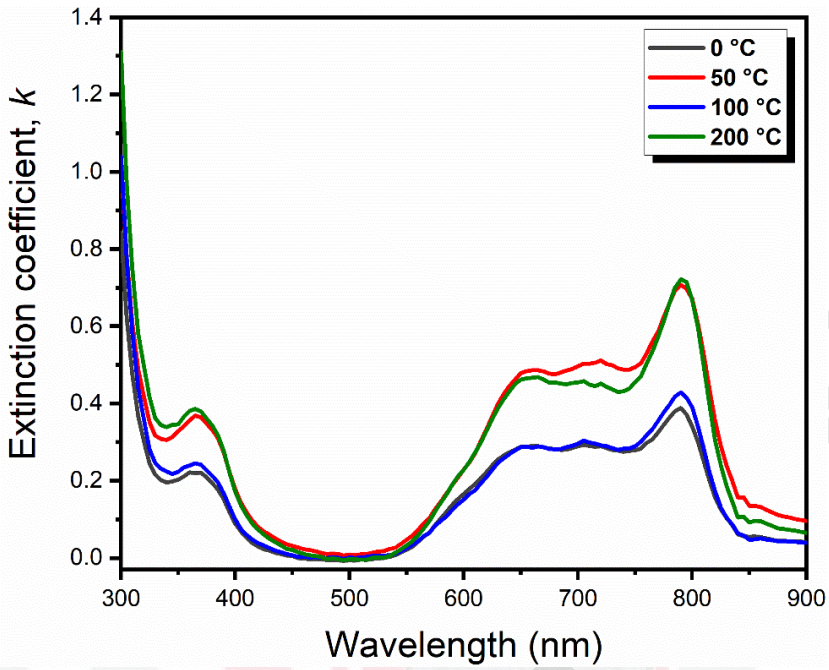


**Figure 4.6:** The extinction coefficient of $F_{16}CuPc$ thin films.

One of the essential parameters of semiconductor films is the optical band gap ($E_g$), which define the threshold for photons to be absorbed. According to Koshy & Menon (2012), the $E_g$ can be determined by using Tauc's equation as follows:

$$\alpha E = \alpha_0 \left(E - E_g\right)^n \quad (8)$$

Where,

$\alpha_0$ = energy-independent constant

$\alpha$ = absorption coefficient

$E$ = energy of incident light

$E_g$ = Optical bandgap energy

$n$ = electronic transition

The type of electronic transition due to absorption can be understood by utilizing exponent value ($n$) in equation (8). An accurate estimation of $n$ and $E_g$ is carried out through mathematical manipulations to equation (8). By taking natural logarithm and derivative, we can obtain:

$$\frac{d\ln(\alpha E)}{dE} = \frac{n}{E - E_g} \tag{9}$$

The approximate value of $E_g$ can be used to determine the value of n from the equation (8):

$$\ln(\alpha E) = \ln(\alpha_0) + \left[n \times \ln(E - E_g)\right] \tag{10}$$

The value of n was determined from the slope of $\ln(\alpha E)$ versus $\ln(E - E_g)$ as shown in Figure 4.7. The value of $n$ was found to be 1/2, which can be found from the slope, indicating the presence of a direct allowed transition between the intermolecular energy levels.

Then, a graph of $(\alpha E)^n$ against $E$ was plotted to determine the accurate value of $E_g$ for $F_{16}CuPc$ thin films, as shown in Figure 4.8. The value of $E_g$ can be determined by extrapolating the linear part of the curves to the horizontal axis where $(\alpha E)^n = 0$. The interception on the axis gives the $E_g$. Table 2 shows the observed energy band gap for $F_{16}CuPc$ thin films.

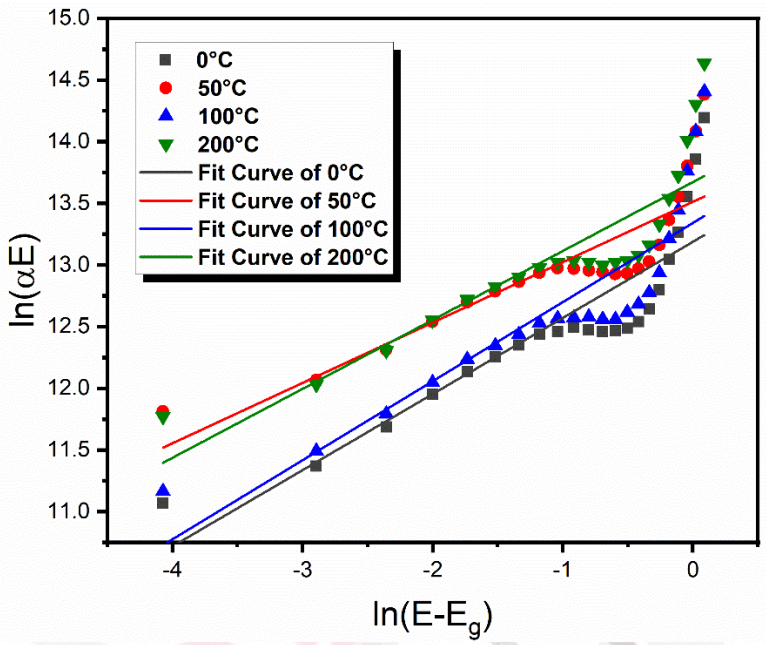


**Figure 4.7:** The graph of ln($\alpha$E) versus ln($E$-$E_g$) of $F_{16}$CuPc thin films.

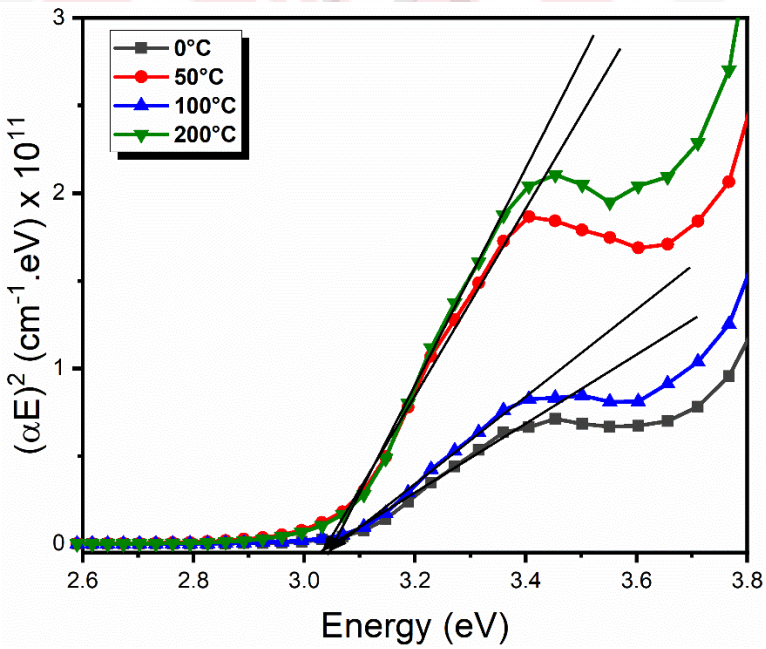


**Figure 4.8:** The graph of $(\alpha E)^n$ versus E for $F_{16}$CuPc thin films.

**Table 2:** The optical band gap energy and transition type of $F_{16}CuPc$ thin films

| Sample | $E_g$ (eV) | Transition type (n) |
|---|---|---|
| As-deposited | 3.05 | Direct allowed (1/2) |
| 50 °C | 3.03 | Direct allowed (1/2) |
| 100 °C | 3.05 | Direct allowed (1/2) |
| 200 °C | 3.04 | Direct allowed (1/2) |

The energy band gap value is compared to a previous study $(3.06 \pm 0.01)$ eV and the value was found in good agreement with the current work (Koshy & Menon, 2012). There is insignificant difference between the reported and experimental energy band gap value. On top of that, the energy band gap value can determine by extrapolating linear lines on a dominant peak to the horizontal axis of the absorbance plot. The intersection of the lines is used to calculate the $E_g$ by using the formula:

$$E_g = \frac{1241}{\lambda} \text{eV} \tag{11}$$

In our case, the intersection is found at 416, 418, and 421 nm, resulting in the average value of optical band gap being 2.97 eV. By comparing both $E_g$ values gained by Tauc's plot and expression, the values do not differ much from the reported value.

**Table 3:** The calculated optical band gap energy

| Sample | Wavelength (nm) | $E_g$ (eV) |
|---|---|---|
| As-deposited | 416 | 2.98 |
| 50 °C | 421 | 2.95 |
| 100 °C | 416 | 2.98 |
| 200 °C | 418 | 2.97 |

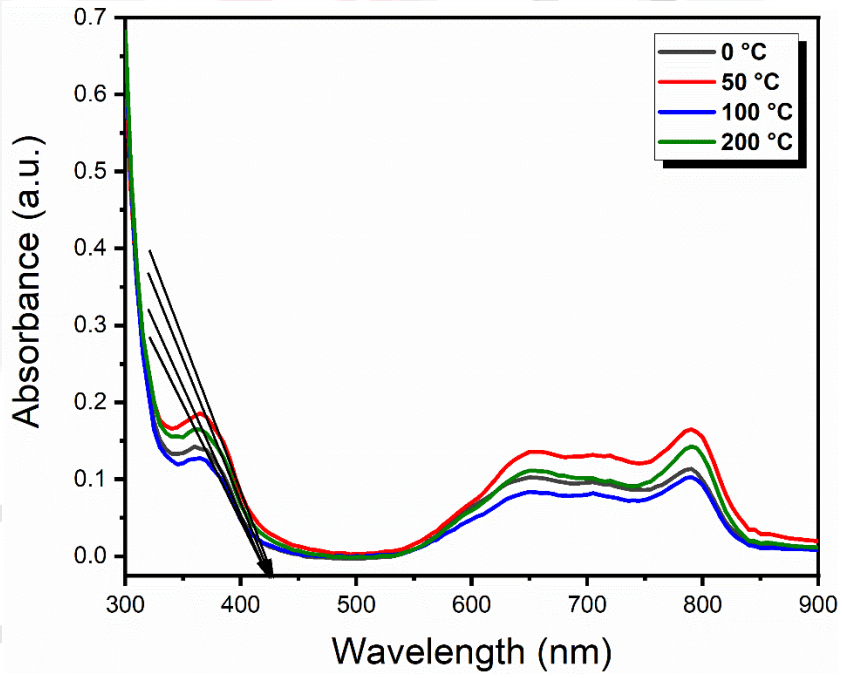


**Figure 4.9:** Plot of absorbance versus wavelength in finding optical band gap energy**.**

Another important parameter is the refractive index. It determines the amount of light being refracted or bent when it passes through a material. The refractive index can be calculated by using formula as follows:

$$R = \frac{(n-1)^2 + k^2}{(n+1)^2 + k^2} \tag{12}$$

This leads to:

$$n = \left(\frac{1+R}{1-R}\right) + \sqrt{\left(\frac{4R}{(1-R)^2}\right) - k^2} \tag{1}$$

Where,

$n$ = refractive index

$R$ = reflectance

$k$ = extinction coefficient

Figure 4.10 depicts the refractive index of $F_{16}CuPc$ thin films, and it shows two broad peaks at 650 nm and 790 nm in the Vis region. Also, there are two peaks in the UV region which are 310 nm and a shoulder at 360 nm, before the graphs decline to 500 nm.

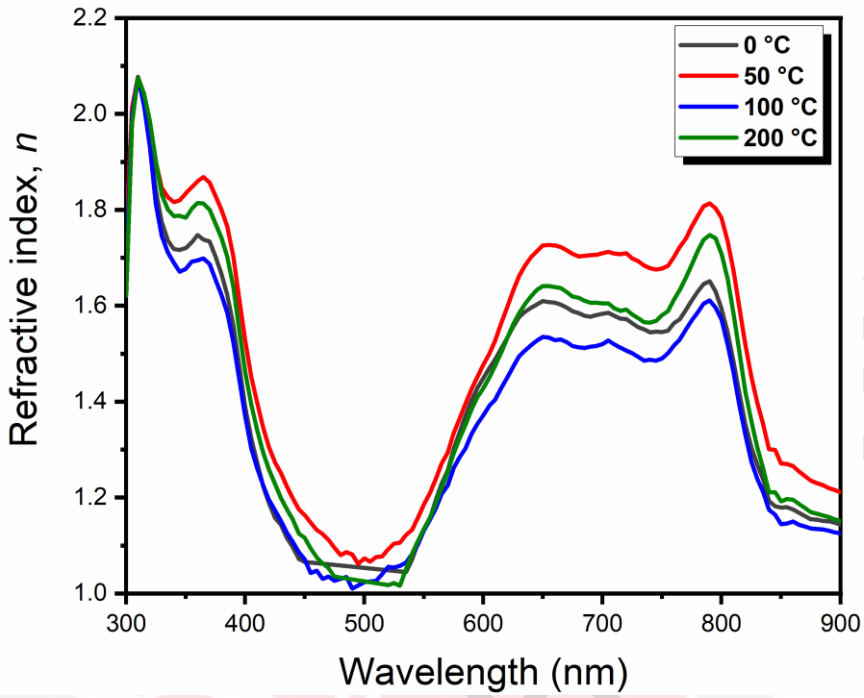


**Figure 4.10:** The refractive index of $F_{16}CuPc$ thin films.

The refractive index and dielectric constant are two crucial parameters highly considered in the characterization of optical properties. The dispersion behavior of the dielectric parameter is represented by its real part ($\varepsilon_r$) while the information on the light dissipation in the films can be obtained from the imaginary part ($\varepsilon_i$) of dielectric constant (Muhammad et al., 2017). According to Koshy & Menon (2012), the dielectric constant parameter and dissipation factor ($\tan\delta$) of $F_{16}CuPc$ films can be determined from the complex dielectric function ($\varepsilon^* = \varepsilon_r + i\varepsilon_i$) as the following:

$$\varepsilon_r = n^2 - k^2 \tag{2}$$

$$\varepsilon_i = 2nk \tag{3}$$

$$\tan\delta = \frac{\varepsilon_i}{\varepsilon_r} \tag{4}$$

Where,

$n$ = refractive index

$k$ = absorption coefficient

$\varepsilon_r$ = real dielectric constant

$\varepsilon_i$ = imaginary dielectric constant

From Figure 4.11, we can see that the real dielectric constant shows two broad peaks in 650 nm to 790 nm. We can also see fluctuations of peaks in the UV range at 310 nm with a shoulder at 365 nm. From Figure 4.12, we can see a peak at 365 nm in the UV region before decreasing to almost 0 at 500 nm. The graph then rises and forms two broad peaks at 665 nm and 790 nm. The following important parameter is the dissipation factor. It can be calculated by the tangent of the angle between $\varepsilon_i$ and $\varepsilon_r$. The dissipation factor indicates the inefficiency of material to hold energy or behave as an insulating material (Shehata et al., 2018). From Figure 4.13, we can see that it has a low dissipation factor at wavelength range within 400 nm to 600 nm and 850 nm. The low value of the dissipation factor means that the material is efficient enough to fabricate high-frequency devices.

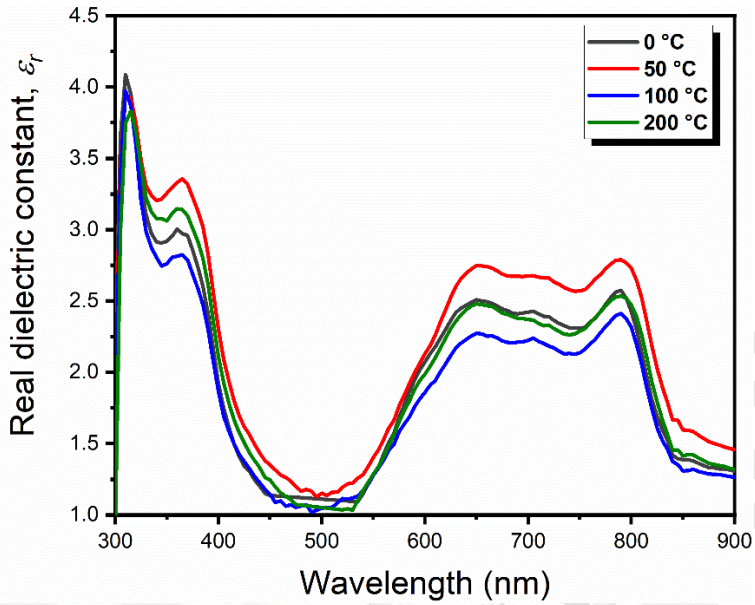


**Figure 4.11:** The real dielectric constant of $F_{16}CuPc$ thin films.

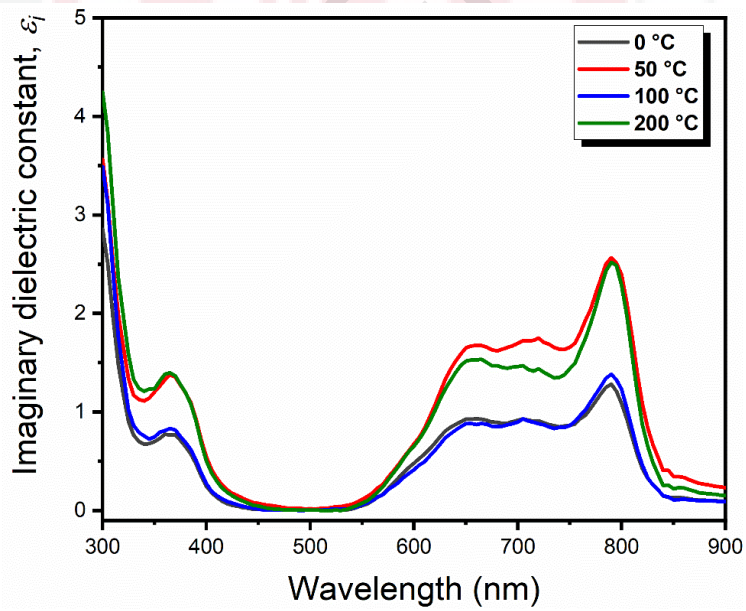


**Figure 4.12:** The imaginary dielectric constant of $F_{16}CuPc$ thin films.

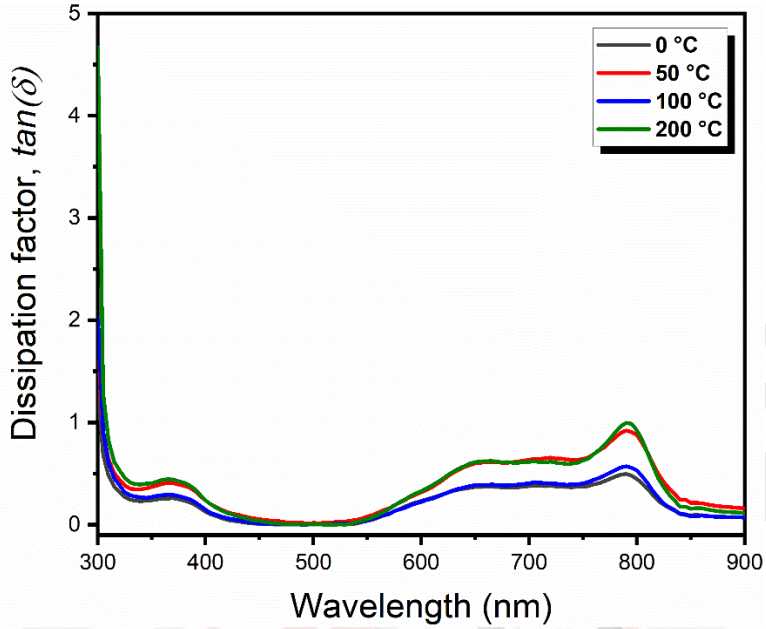


**Figure 4.13:** The dissipation factor spectra of $F_{16}CuPc$ thin films.

Optical conductivity is the extension of electrical transport, which a measure of frequency response when the material is exposed to light (Shehata et al., 2018). Real and imaginary optical conductivity ($\sigma^* = \sigma_r + i\sigma_i$) can be investigated by using the following formula:

$$\sigma_r = \omega \varepsilon_0 \varepsilon_i \quad (5)$$

$$\sigma_i = \omega \varepsilon_0 \varepsilon_r \quad (6)$$

Where,

$\sigma_r$ = real optical conductivity

$\sigma_i$ = imaginary optical conductivity

$\omega$ = angular frequency

$\varepsilon_0$ = free space permittivity ($8.85 \times 10^{-12}$ F m$^{-1}$)

Figure 4.14 shows the real conductivity spectra of $F_{16}CuPc$ thin films. We can notice that the real conductivity has its peak in the UV region at 361 nm, and there is also a peak at 788 nm with a broad shoulder near 650 nm. As seen in Figure 4.15, the imaginary conductivity depicts a sharp peak in the earlier range of the UV region before declining and forming a shoulder at 360 nm. The $F_{16}CuPc$ thin film shows low imaginary conductivity in the Vis region before increasing at 635 nm to 790 nm. The value keeps on decreasing in the IR region.

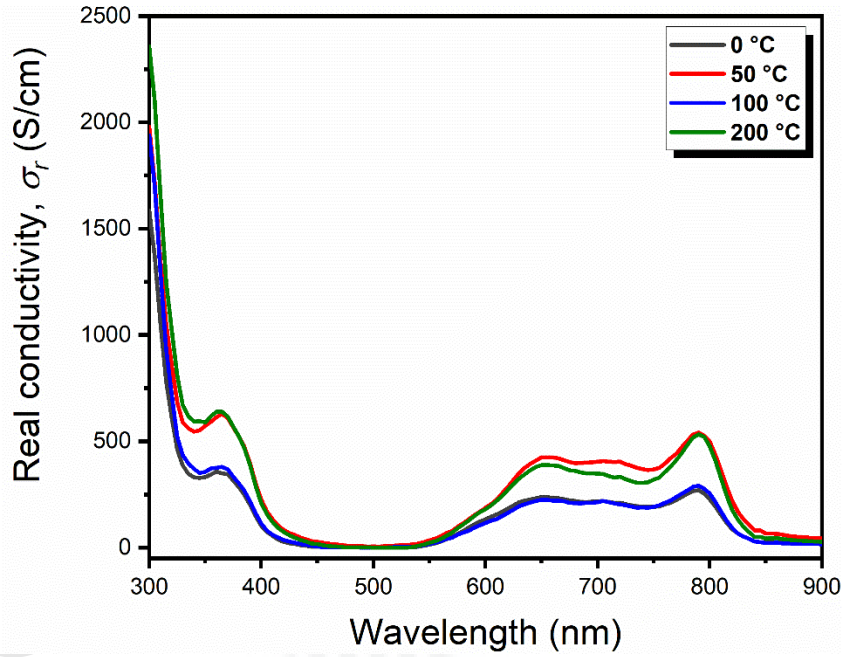


**Figure 4.14:** The real conductivity versus wavelength of $F_{16}CuPc$ thin films.

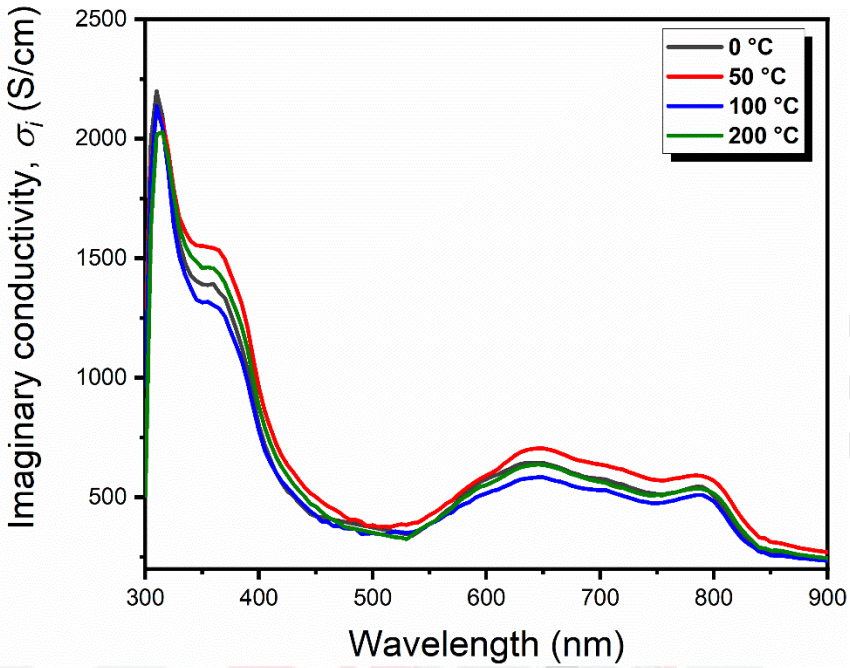


**Figure 4.15:** The imaginary conductivity versus wavelength of $F_{16}CuPc$ thin films.

### 4.3 Structural Properties

X-ray diffraction (XRD) is used in the range from 20° to 80° to determine the structural properties of $F_{16}$CuPc powder. The data is then analyzed by using X'Pert Highscore Plus software. The XRD pattern of $F_{16}$CuPc powder is shown in Figure 16.

As seen in Figure, the $F_{16}$CuPc powder displayed a crystallized phase at $2\theta$ = 22.69° and 28.38°, which shows a crystallized phase. The Full Width at Half Maximum (FWHM) of $F_{16}$CuPc powder is 0.6336 and 0.5544. Based on Figure 4.16, one can see that the $F_{16}$CuPc thin film being annealed for 100°C for 30 mins displayed an amorphous phase. Theoretically, a thin film deposited by a thermal evaporation has high possibility to form a crystalline film. However, there is no peaks displayed in the XRD spectra for the evaporated sample indicating the amorphous film. According to Ye et al. (2006), increasing the substrate temperature enhances the crystallinity of the thin film.

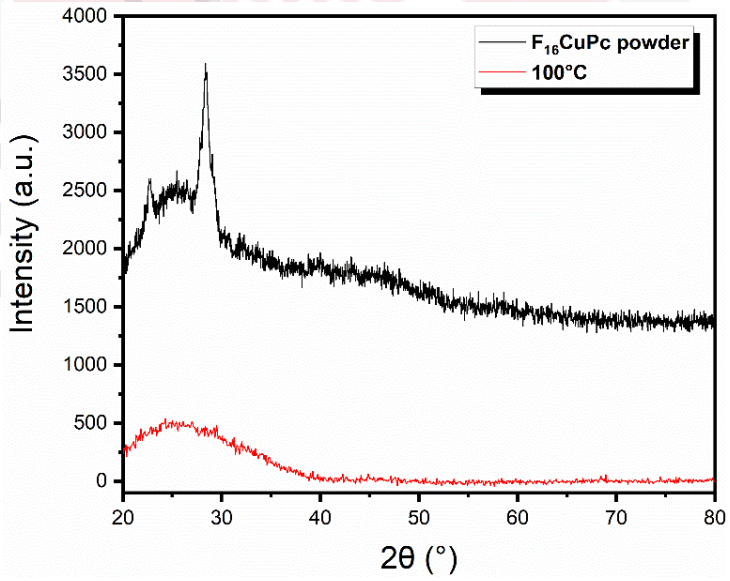


**Figure 4.16:** The XRD analysis for as deposited and annealed at 100°C $F_{16}$CuPc thin films.

There are many factors that could lead to the formation of an amorphous film, which somehow contribute to challenges in this research work. Firstly, the inability to optimized the thermal evaporator settings used in this work. For example, there is no indicator to control the deposition rate, which is very crucial in the formation of crystalline film. The short distance between the tungsten source and the glass substrates (~ 5cm) might be another factor of the failure to form a crystalline film. According to Yadav et al. (2012), growth temperature and the low deposition rate extend the diffusion length of molecules prior to burial beneath the approaching stream of molecules, hence enhancing crystallinity.

## 4.4 Morphological properties

Atomic Force Microscopy (AFM) is used to characterize the surface morphologies and surface roughness of $F_{16}CuPc$ thin films. These figures in the following are the AFM images of $F_{16}CuPc$ thin films in a 2 $\mu$m × 2$\mu$m area.

Surface roughness is obtained based on $R_q$'s value, where $R_q$ is the surface's root mean square (RMS) height. The root mean square (RMS) was obtained using the AFM instrument for each sample. The bigger the value of RMS, the rougher the surface. Table 4 shows the RMS value of the $F_{16}CuPc$ thin films.

**Table 4:** The RMS value of $F_{16}CuPc$ thin films

| Sample | RMS (nm) |
|---|---|
| As-deposited | 5.88 |
| 50 °C | 6.84 |
| 100 °C | 7.36 |
| 200 °C | 9.54 |

Figure 4.17 displays the AFM images of $F_{16}CuPc$ thin films. From Table 4, the $F_{16}CuPc$ thin films are seen to exhibit a higher RMS value as the temperature of the organic films increases. The grain size appears to be elongated, which leads to improving crystallinity (Yadav et al., 2012).

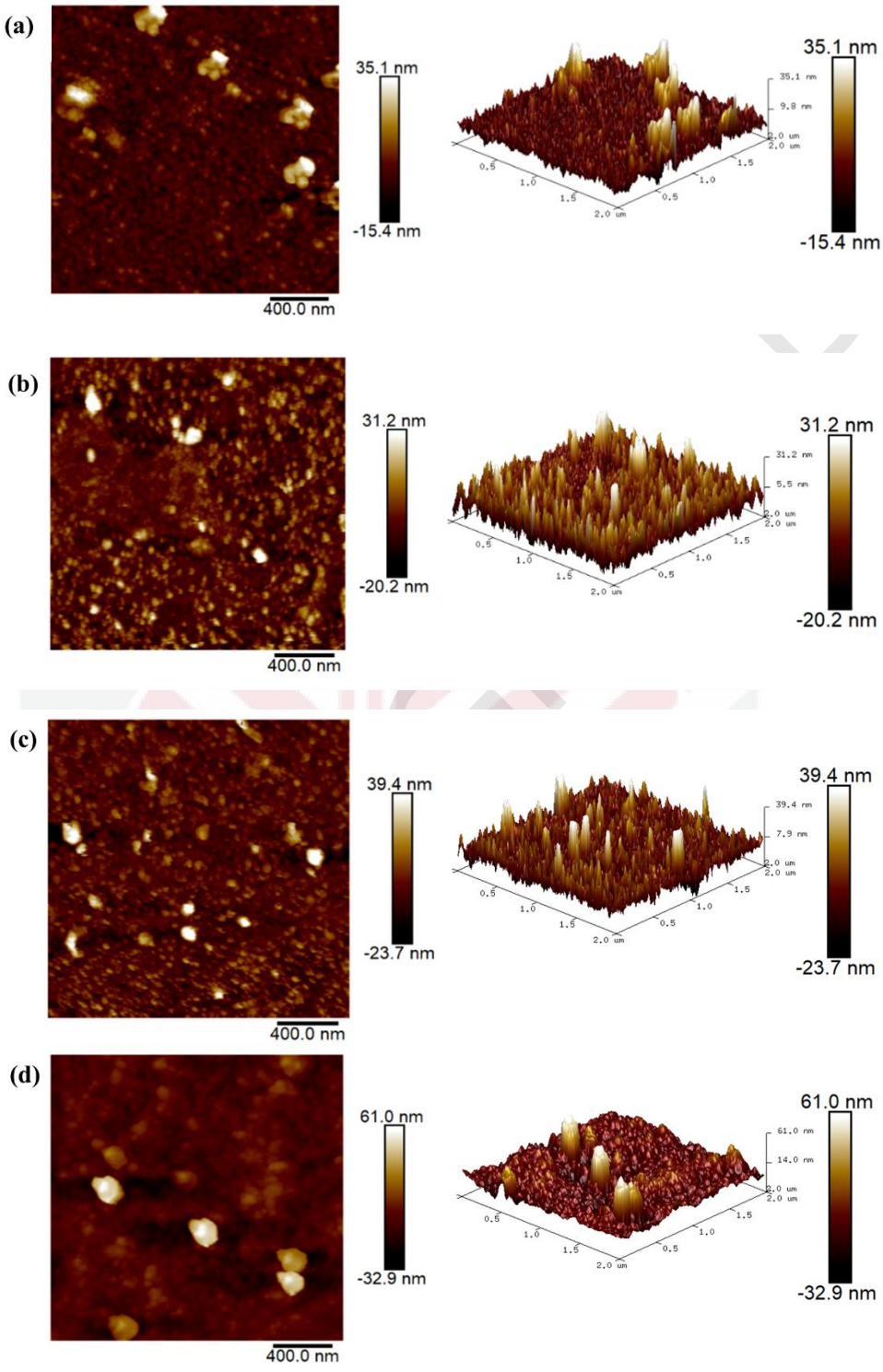


**Figure 4.17:** 2 and 3-dimensional structure of $F_{16}CuPc$ thin films **(a)** As-deposited, **(b)** 50 °C, **(c)** 100 °C and **(d)** 200 °C.

# CHAPTER 5

# CONCLUSION

## 5.1 Conclusion

In this study, $F_{16}$CuPc thin films were successfully deposited by thermal evaporation method. An extensive optical parameters, as well as structural, and morphological properties of $F_{16}$CuPc thin films were characterized and analyzed. The deposition time was fixed at 60 s and controlled at 38 A with 15 mg of $F_{16}$CuPc powder. The deposited thin films were then annealed to 50°C, 100°C, and 200°C for 30 minutes. A comparative study of the aforementioned properties was carried out on the effect of annealing temperature of the deposited $F_{16}$CuPc thin film.

Various optical parameters such as absorbance, absorption coefficient, transmittance, reflectance, refractive index, dissipation factor, extinction coefficient, dielectric constant, and optical conductivity were studied in the UV-Vis-NIR range of the light spectrum. The study shows that $F_{16}$CuPc thin films were absorbed well in the UV and Vis range, with two sharp peaks at 360 nm and 789 nm as well as a shoulder at 650 nm, corresponding to $\pi$-$\pi^*$ transitions, respectively. This study has proved that no significant effect on temperature variations for optical properties of $F_{16}$CuPc thin films. The $F_{16}$CuPc thin films presented a high extinction coefficient in the Vis region, making them suitable for light sensing application. The electronic transition in $F_{16}$CuPc thin films was found to be direct allowed (1/2) and was used in Tauc's equation to estimate optical energy band gap, $E_g$. It was found that the $E_g$ value gained from Tauc's equation, ($3.04 \pm$

0.01) eV is close enough to the value gained by extrapolating the plot of absorbance to the horizontal axis, which is 2.97 eV.

Structural properties have been analysed using XRD analysis, which shows the $F_{16}CuPc$ powder is in the crystalline nature. However, the study depicts a formation of an amorphous phase after deposited via thermal evaporation for annealed $F_{16}CuPc$ thin film. This might be due to the poor optimization during the deposition process.

Despite the inability to acquire a high cyrstalline $F_{16}CuPc$ thin film, the AFM morphological study of $F_{16}CuPc$ thin films shows that the surface roughness increases as the annealing temperature increases. This proved by the formation of grains which then can lead to improve the crystallinity of the thin film.

## 5.2 Future work

1. The deposition process should be further optimized by using a suitable distance between the source and the substrates, and the deposition rate should be low and in control to get a better structure of $F_{16}CuPc$ thin films.
2. The effect of thermal annealing on the other properties should be done to enhance the understanding of $F_{16}CuPc$ thin films.

## REFERENCES


Akamatu, H., Inokuchi, H., & Mastunaga, Y. (1956). Semiconductors with High Conductivity . *Bulletin of the Chemical Society of Japan*, *29*(2), 213–218.

Basir, A., Alzahrani, H., Sulaiman, K., Muhammadsharif, F. F., Mahmoud, A. Y., Bahabry, R. R., Alsoufi, M. S., Bawazeer, T. M., & Ab Sani, S. F. (2021). An investigation on the optical parameters of TPD:Alq3 composite thin films. *Physica B: Condensed Matter*, *606*. https://doi.org/10.1016/j.physb.2021.412816

Çavuş, H. K., Voigt, M. M., & Şahingöz, R. (2013). Optical and electrical properties of new organic thin film. *Journal of Materials Science: Materials in Electronics*, *24*(12), 4833–4838. https://doi.org/10.1007/s10854-013-1483-9

Collins, R. A., & Mohammed, K. A. (1986). Electrical, structural and gas sensing properties of zinc phthalocyanine thin films. *Thin Solid Films*, *145*(1), 133–145. https://doi.org/10.1016/0040-6090(86)90260-9

El-Nahass, M. M., El-Gohary, Z., & Soliman, H. S. (2003). Structural and optical studies of thermally evaporated CoPc thin films. *Optics and Laser Technology*, *35*(7), 523–531. https://doi.org/10.1016/S0030-3992(03)00068-9

El-Nahass, M. M., Zeyada, H. M., Aziz, M. S., & El-Ghamaz, N. A. (2004). Structural and optical properties of thermally evaporated zinc phthalocyanine thin films. *Optical Materials*, *27*(3), 491–498. https://doi.org/10.1016/j.optmat.2004.04.010

Hideki Shirakawa, B., Louis, E. J., Macdiarmid, A. G., W A N K Chiang, C. H., & HEEGERt, A. J. (1977). *Synthesis of Electrically Conducting Organic Polymers : Halogen Derivatives of Polyacetylene, (CH)*.

Jiang, X., Dai, J., Wang, H., Geng, Y., & Yan, D. H. (2007). Organic photovoltaic cells using hexadecafluorophthalocyaninatocopper (F16CuPc) as electron acceptor material. *Chemical Physics Letters*, *446*(4–6), 329–332. https://doi.org/10.1016/j.cplett.2007.08.042

Kallmann, H., & Pope, M. (1960). *© 1960 Nature Publishing Group*.

Karan, S., & Mallik, B. (2007). Effects of annealing on the morphology and optical property of copper (II) phthalocyanine nanostructured thin films. *Solid State Communications*, *143*(6–7), 289–294. https://doi.org/10.1016/j.ssc.2007.05.043

Kietzke, T. (2007). Recent advances in organic solar cells. *Advances in OptoElectronics*, *2007*. https://doi.org/10.1155/2007/40285

Kippelen, B., & Brédas, J. L. (2009). Organic Photovoltaics. In *Energy and Environmental Science* (Vol. 2, Issue 3, pp. 251–261). https://doi.org/10.1039/b812502n

Köhler, A., & Bässler, H. (2015). The Electronic Structure of Organic Semiconductors. In *Electronic Processes in Organic Semiconductors* (pp. 1–86). https://doi.org/10.1002/9783527685172.ch1

Koshy, R., & Menon, C. S. (2012). Effect of vacuum annealing on the optoelectric and morphological properties of F16CuPc thin films. *E-Journal of Chemistry*, *9*(1), 294–300. https://doi.org/10.1155/2012/101686

Kuehne, A. J. C., & Gather, M. C. (2016). Organic Lasers: Recent Developments on Materials, Device Geometries, and Fabrication Techniques. *Chemical Reviews*, *116*(21), 12823–12864. https://doi.org/10.1021/acs.chemrev.6b00172

Lü, B., Riede, M., & Leo, K. (2007). *Doping of organic semiconductors*. https://doi.org/10.1002/pssa.201228310

Mehta, J., Brit, S. F. J., Secker, P., Guile, E., St, A. E., John, R. M., Winans, J. G., Davies, D. E., Fitch, R. K., Ecker, G., & Muller, K. G. (1957). Bulk Conductivity in Organic Crystals. In *Proc. Imt. Elu. Eng* (Vol. 8).

Muhammad, F. F., Yahya, M. Y., Aziz, F., Rasheed, M. A., & Sulaiman, K. (2017). Tuning the extinction coefficient, refractive index, dielectric constant and optical conductivity of Gaq3 films for the application of OLED displays technology. *Journal of Materials Science: Materials in Electronics*, *28*(19), 14777–14786. https://doi.org/10.1007/s10854-017-7347-y

Nyokong, T. (2011). Desired properties of new phthalocyanines for photodynamic therapy. *Pure and Applied Chemistry*, *83*(9), 1763–1779. https://doi.org/10.1351/PAC-CON-10-11-22

Rasmussen, S. C. (2017). The Early History of Polyaniline: Discovery and Origins. *An International Journal of the History of Chemistry*, *1*(2), 99–109. https://doi.org/10.13128/substantia-30

Reineke, S., Lindner, F., Schwartz, G., Seidler, N., Walzer, K., Lüssem, B., & Leo, K. (2009). White organic light-emitting diodes with fluorescent tube efficiency. *Nature*, *459*(7244), 234–238. https://doi.org/10.1038/nature08003

Ren, H., Chen, J. De, Li, Y. Q., & Tang, J. X. (2021). Recent Progress in Organic Photodetectors and their Applications. *Advanced Science*, *8*(1), 1–23. https://doi.org/10.1002/advs.202002418

Ren, J., Meng, S., Wang, Y.-L., Ma, X.-C., Xue, Q.-K., & Kaxiras, E. (2011). Properties of copper (fluoro-)phthalocyanine layers deposited on epitaxial graphene. *THE JOURNAL OF CHEMICAL PHYSICS*, *134*, 194706. https://doi.org/10.1063/1.3590277

Rongbin, Y. E., Baba, M., & Mori, K. (2005). High-performance air-stable ambipolar organic thin-film transistor based on F16CuPc and CuPc. *Japanese Journal of Applied Physics, Part 2: Letters*, *44*(16–19), 4–7. https://doi.org/10.1143/JJAP.44.L581

Sakamoto, K., & Ohno-Okumura, E. (2009a). Syntheses and functional properties of phthalocyanines. *Materials*, *2*(3), 1127–1179. https://doi.org/10.3390/ma2031127

Sakamoto, K., & Ohno-Okumura, E. (2009b). Syntheses and functional properties of phthalocyanines. *Materials*, *2*(3), 1127–1179. https://doi.org/10.3390/ma2031127

Shehata, M. M., Kamal, H., Hasheme, H. M., El-Nahass, M. M., & Abdelhady, K. (2018). Optical spectroscopy characterization of zinc tetra pyridel porphine (ZnTPyP) organic thin films. *Optics and Laser Technology*, *106*, 136–144. https://doi.org/10.1016/j.optlastec.2018.03.032

Sridevi, B. R., Hoskeri, P. A., & Joseph, C. M. (2021). Effect of annealing on the optical, structural and electrochromic properties of vacuum evaporated manganese phthalocyanine thin films. *Thin Solid Films*, *723*. https://doi.org/10.1016/j.tsf.2021.138584

Van Staden, J. K. F. (2015). Application of phthalocyanines in flow- and sequential-injection analysis and microfluidics systems: A review. In *Talanta* (Vol. 139, pp. 75–88). https://doi.org/10.1016/j.talanta.2015.02.026

Wang, Y., Wu, K., Kröger, J., & Berndt, R. (2012). Review article: Structures of phthalocyanine molecules on surfaces studied by STM. In *AIP Advances* (Vol. 2, Issue 4). American Institute of Physics Inc. https://doi.org/10.1063/1.4773458

Witte, G., & Wöll, C. (2004). Growth of aromatic molecules on solid substrates for applications in organic electronics. *Journal of Materials Research*, *19*(7), 1889–1916. https://doi.org/10.1557/JMR.2004.0251

Yadav, S., Kumar, P., & Ghosh, S. (2012). Optimization of surface morphology to reduce the effect of grain boundaries and contact resistance in small molecule based thin film transistors. *Applied Physics Letters*, *101*(19). https://doi.org/10.1063/1.4766913

Ye, R., Baba, M., Ohishi, Y., Mori, K., & Suzuki, K. (2006). On the correlation between morphology and electronic properties of fluorinated copper phthalocyanine (F16CuPc) thin films. *Molecular Crystals and Liquid Crystals*, *444*(July 2013), 203–210. https://doi.org/10.1080/15421400500364972

Ye, R., Baba, M., Ohta, K., & Suzuki, K. (2010). Effects of thermal annealing on structure, morphology and electrical properties of F16CuPc/α6T heterojunction thin films. *Solid-State Electronics*, *54*(7), 710–714. https://doi.org/10.1016/j.sse.2010.03.014

Ye, R., Baba, M., Suzuki, K., & MOri, K. (2008). *Structure and morphology of CuPc and F16CuPc pn heterojunction*. Applied Surface Science. https://www.researchgate.net/publication/257027513_Structure_and_morphology_of_CuPc_and_F16CuPc_pn_heterojunction

Zhang, G., Ma, F., Wang, L., Sun, B., Zhao, J., & Liu, F. (2019). Synthesis, characterization of copper perfluorophthalocyanine (F16CuPc) and its application in organic thin-film transistors. *Materiali in Tehnologije*, *53*(6), 827–831. https://doi.org/10.17222/mit.2018.260

Zschieschang, U., & Klauk, H. (2019). Organic transistors on paper: A brief review. *Journal of Materials Chemistry C*, *7*(19), 5522–5533. https://doi.org/10.1039/C9TC00793H